




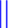


Detecting superfluid transition in the pulsar core

Partha Bagchi ¹ *, Biswanath Layek ² †, Dheeraj Saini ³ ‡, Anjishnu Sarkar ³ §,
Ajit M. Srivastava ⁴ ¶ and Deepthi Godaba Venkata ² ||

¹ School of Physical Sciences, National Institute of Science Education and Research, Bhubaneswar, India.

² Department of Physics, Birla Institute of Technology and Science, Pilani-333031, India.

³ Physics Department, The LNM Institute of Information Technology, Jaipur-302031, India.

⁴ Institute of Physics, Sachivalaya Marg, Bhubaneswar-751005, India.

ABSTRACT

It is believed that the core of a neutron star can be host to various novel phases of matter, from nucleon superfluid phase to exotic high baryon density quantum chromodynamics (QCD) phases. Different observational signals for such phase transitions have been discussed in the literature. Here, we point out a unique phenomenon associated with phase transition to a superfluid phase, which may be the nucleon superfluid phase or a phase like the CFL phase, allowing for superfluid vortices. In any superfluid phase transition, a random network of vortices forms via the so-called Kibble-Zurek mechanism, which eventually mostly decays away, finally leaving primarily vortices arising from the initial angular momentum of the core. This transient, random vortex network can have a non-zero net angular momentum for the superfluid component, which will generally be oriented in an arbitrary direction. This is in contrast to the final vortices, which arise from initial rotation and hence have the initial angular momentum of the neutron star. The angular momentum of the random vortex network is balanced by an equal and opposite angular momentum in the normal fluid due to the conservation of angular momentum, thereby imparting an arbitrarily oriented angular momentum component to the outer shell of the neutron star. This will affect the pulse timing and pulse profile of a pulsar. These changes in the pulses will decay away in a characteristic manner such that the random vortex network decays, obeying specific scaling laws leading to universal features for the detection of superfluid transitions occurring in a pulsar core.

Key words: pulsar, superfluid transition, vortices, Kibble-Zurek mechanism, pulse profile, precession, phase transition.

1 INTRODUCTION

Physics of neutron stars has been a very exciting area of research, with their cores having matter at extreme baryon density. There has been an explosion of interest in neutron stars with the direct detection of gravitational waves by LIGO/Virgo coming from binary neutron star (BNS) merger events. The properties of neutron star cores directly affect gravitational waveform, especially during the last stages of merger. There have been numerous investigations probing the possibility of detecting such effects in the presence of high baryon density QCD phases, e.g., the deconfined QCD phase in the neutron star cores (Bauswein et al. 2019; Most et al. 2019) (see also Ref. (Demircik et al. 2022; Radice et al. 2017)). However, for a nucleonic superfluid phase, there is convincing evidence of such a phase in the

neutron star’s inner crust and core. The existence of such a superfluid phase in the neutron star interior was first hypothesized by Migdal (1959). It was subsequently proposed that such a superfluid phase may be responsible for the observed decrease in the slow-down rate of the Vela pulsar in its post-glitch relaxation stage (Baym et al. 1969). Superfluid phase is now believed to provide a natural explanation of pulsar glitches which can arise from the de-pinning of superfluid vortices (Anderson & Itoh 1975; Ruderman 1976). Nucleon superfluidity inside the neutron star’s core also directly affects the neutron star cooling. The observed rapid cooling of the neutron star in Cassiopeia A (Cas A) supports the hypothesis of nucleon superfluid phase in the neutron star’s core (Shternin et al. 2022). Note that after the discovery of the neutron star in Cas A (Hughes et al. 2000), this star is found to be among a few isolated neutron stars with a well-determined age and a reliable surface temperature, thus allowing for modelling of its thermal evolution and the determination of its interior properties. Page et al. (2011) and Shternin et al. (2011) claimed that enhanced neutrino emission caused by the breaking and formation of neutron Cooper

* E-mail: parphy@niser.ac.in, parphy85@gmail.com

† E-mail: layek@pilani.bits-pilani.ac.in

‡ E-mail: 23pph001@lnmiit.ac.in

§ E-mail: anjishnu@lnmiit.ac.in

¶ E-mail: ajit@iopb.res.in

|| E-mail: p20210075@pilani.bits-pilani.ac.in

pairs in the 3P_2 channel is responsible for the rapid cooling of the neutron star in Cas A.

Note that, superfluidity in condensed matter systems has been observed for more than hundred years (e.g. in ${}^4\text{He}$, and later in ${}^3\text{He}$). Quantized vortices in superfluid helium have also been routinely studied in laboratory experiments for a long time. Regarding superfluid phase arising from Cooper pairing of nucleons, the experimental evidence from laboratory experiments comes from the effects of pairing correlations in finite nuclei where it is manifested in the odd-A - even-A staggering of the binding energies (Sedrakian & Clark 2019). Such Cooper pairing of nucleons in the interior of neutron stars can also affect the cooling rate of neutron stars (Shternin et al. 2022; Page et al. 2011). One of the observational (indirect) evidence for superfluid vortices in a nucleonic superfluid (arising from Cooper pairing of nucleons) has been in terms of pulsar glitches (see the recent work (Allard & Chamel 2024) for further evidence of superfluid vortices in the neutron star interior).

In this paper we will provide a novel phenomenon occurring in a neutron star core which undergoes a superfluid phase transition. Our discussion will only utilize the superfluid nature of the transition, and hence will equally apply to conventional nucleon superfluid phase, as well as the exotic extreme baryon density QCD phases such as the color-flavor locked (CFL) phase which is also expected to be a superfluid phase of the diquark condensate. There have been many investigations of the effects of phase transitions in the neutron star core, and its observational signatures. Some of the signals are, effects on the cooling rate of neutron stars (see, e.g (Page et al. 2011) for nucleon superfluid case and (Alford et al. 2008; Rajagopal 2002) for exotic high baryon density QCD phases), change in the moment of inertia of the core due to change in the free energy of new phase (Heiselberg & Hjorth-Jensen 1998), and the effects of density fluctuations produced during a phase transition on the pulsar rotational dynamics (Bagchi et al. 2015). In the investigations of effects of phase transition induced density fluctuations, some of us had also discussed specific case of superfluid phase transitions, by focusing on the random density fluctuations produced by superfluid vortex network (Bagchi et al. 2015). However, the fact that superfluid vortices involve fluid circulation was not utilized in those discussions, only the effects on the energy density fluctuations was considered. Here we focus on the fluid circulation associated with the vortex network and show that it leads to specific observational signals.

Our discussion will be specific to a pulsar undergoing a superfluid phase transition, which can be the nucleon superfluid phase, or a phase like CFL phase, allowing for superfluid vortices. It is well established that in a superfluid phase transition, a random network of vortices forms, via the so called Kibble-Zurek mechanism (Kibble 1976; Zurek 1996). This has been seen in laboratory experiments and is well understood using a picture of correlation domain formation during a phase transition. As the phase of the superfluid condensate randomly varies from one domain to another, it leads to formation of vortices at junctions of various domains around which the phase winds non-trivially. The resulting vortex network shows universal properties, and decays away with specific scaling exponent (Brandenberger 1994; Liu et al. 2021). This is the picture in the absence of any initial rotation present for the matter undergoing superfluid transition. In

the presence of initial rotation, the Kibble-Zurek mechanism has to be modified, as apart from the random vortex network, which are randomly oriented, extra vortices need to be created to carry the initial net angular momentum of the fluid. This modified mechanism was proposed by some of us in Ref. (Dave & Srivastava 2019), and we will incorporate these considerations in discussing formation of vortex network here.

The random vortex network formed by the Kibble-Zurek mechanism (with due consideration of initial rotation) will eventually mostly decay away, finally leaving primarily vortices arising from initial angular momentum of the neutron star. As vortices in this random vortex network are randomly oriented, in general there can be a non-zero net angular momentum for the superfluid component, which can be oriented in an arbitrary direction. Important thing is that the direction of this net angular momentum will be completely independent of the original angular momentum of the neutron star. Along with this random vortex network there will also be extra vortices which arise from initial rotation. These extra vortices will carry the initial angular momentum of the neutron star. (Das et al. 2017; Dave & Srivastava 2019) had pointed out an important aspect of the formation of the random vortex network, which needs to be incorporated in the discussions of the Kibble-Zurek mechanism, especially in relation to experimental observations of fluid circulation. This involves implementation of angular momentum conservation, arising from strict local linear momentum conservation, for the random vortex network formation. We will discuss it below in detail. Basically one finds that the angular momentum carried by the random superfluid vortex network has to be balanced by an equal and opposite angular momentum in the normal fluid. The end result is that the arbitrarily oriented angular momentum component of the vortex network is finally transferred (with opposite direction) to the outer shell of neutron star. This extra angular momentum, though very tiny, will induce a wobbling of the neutron star, in addition to affecting its spin. This can be detected for pulsars with high precision measurements of the pulse timings and the pulse profile changes.

An important aspect of this signal, which can distinguish it from other physical effects, arises from the fact that the random vortex network decays obeying specific scaling laws. (This will occur as vortices and anti-vortices annihilate, and also as vortices pointing in different directions re-orient.) Thus the perturbations in the pulse timings and the pulse profile changes will also decay in very specific manner consistent with those scaling laws. Such universal features in observed pulses may give robust signals of superfluid phase transitions occurring in pulsar cores. (In this context we mention that, although there is a strong evidence that the neutron star in Cassiopeia A may be undergoing superfluid phase transition (Shternin et al. 2022; Page et al. 2011), it will be difficult to test our proposed mechanism for this case as there has not been any detection of pulses from this neutron star (Ho & Heinke 2009). A pulsar at similar stage of evolution will be an ideal candidate for testing the predictions of the mechanism proposed here.)

The paper is organized in the following manner. In section 2, we discuss basic physics of superfluid phases expected in the neutron star core. Here we will discuss conventional nucleon superfluidity as well as the superfluidity expected in extreme baryon density QCD phases with (colored) diquark

condensate. In Section 3 we will discuss the Kibble-Zurek mechanism for the formation of random vortex in a superfluid transition. Here we will also discuss the considerations from Ref. (Das et al. 2017; Dave & Srivastava 2019) for the modifications in Kibble-Zurek mechanism needed to account for extra vortices needed for systems with initial rotation, e.g. rotating neutron star. In Section 4, we will discuss estimates of net, randomly oriented, angular momentum arising from the random vortex formed during superfluid transition. Section 5 presents discussion of observational consequences of this extra, randomly oriented, angular momentum on pulsar timing as well as pulse profile. We conclude in section 6 with discussion of various uncertainties in our estimates, as well as the strengths of these predictions in terms of universal features of these estimates.

2 SUPERFLUID PHASES IN THE CORE OF A NEUTRON STAR

Here we will discuss basic physics of superfluid phases expected in the neutron star core. We first discuss conventional nucleon superfluidity, basic picture and estimates of relevant correlation length etc. Next we will discuss basic physics of color superconducting QCD phases expected to occur at extreme baryon density. Some of these phases, such as the color flavor locked (CFL) phase, display superfluidity and we will present model estimates of correlation length for this case.

2.1 Nucleon Superfluidity

The theoretical studies of neutron star physics for the last few decades, supplemented with pulsar glitch data (Manchester 2017), led to the belief in the existence of neutron superfluidity in the interior of neutron stars (Baym et al. 1969). Below the outer crust region lies a few hundred meters thick inner crust of mass density $0.002\rho_0 \leq \rho \leq 0.8\rho_0$ ($\rho_0 = 2.8 \times 10^{14}$ g cm⁻³ is the saturation density of nuclear matter.), which is believed to host the neutron superfluidity in the 1S_0 BCS pairing state. The core of about 10 km radius with density $\rho \geq \rho_0$ may contain neutron superfluidity in 3P_2 state and a proton superconductor in 1S_0 state. Depending on the density of the core region, as we discussed earlier, even more exotic QCD phases can appear in the superfluid form, viz., CFL, LOFF and 2SC color superconductivity, etc. The presence of neutron superfluidity in the interior of the neutron star is one of the main ingredients of the proposed superfluid-vortex model for pulsar glitches (Anderson & Itoh 1975; Ruderman 1976). The basic idea of this model is the sharing of excess angular momentum carried by the pinned superfluid vortices in the inner crust to the co-rotating outer (rigid) crust - core region of the star (see the reviews (Haskell & Melatos 2015; Antonopoulou et al. 2022) on pulsar glitches and various related issues). The success of the vortex model in explaining various features of pulsar glitches thus provides indirect evidence of superfluidity in the neutron star interior (Baym et al. 1969; Anderson & Itoh 1975; Ruderman 1976).

Here, we briefly recall the theoretical arguments in favour of the formation of nucleon superfluidity inside a neutron star, supplemented with the values of relevant superfluid parameters obtained from various model calculations. The ef-

fective nucleon-nucleon interaction is a combination of short-range repulsion and a long-range attraction. As a result, two distinct types of neutron superfluidity are expected to occur in the interior. A few femtometer inter-particle distance in the inner-crust region favours the long-range attractive interaction, resulting in 1S_0 neutron superfluidity. At higher densities ($\geq \rho_0$), it's a competition between a short-range repulsion and a long-range attraction, leading to 3P_2 pairing. The superfluid parameters, viz., the superfluid gap Δ , the critical temperature T_c , etc., have been estimated using various many-body approaches (In this context, see the very informative reviews (Dean & Hjorth-Jensen 2003; Sedrakian & Clark 2019) on the quantitative understanding of superfluidity through the microscopic pairing theories in various nuclear systems, including the system of neutron-star interiors.). These parameters vary with the baryon density. The various studies suggest that the superfluid critical temperature in the core region lies in the (0.1 - 0.5) MeV range. The cooling mechanism of neutron stars has been studied and discussed extensively in the literature; see Refs. (Yakovlev & Pethick 2004; Yakovlev et al. 2005; Page et al. 2006). The above studies suggest the star's typical interior temperature to be about $T \simeq 0.01$ MeV (Yakovlev & Pethick 2004), which is well below the critical temperature and relatively uniform in the inner region of the star because of the high thermal conductivity of the degenerate quantum liquid. Though our discussion will relate to vortex formation during the superfluid phase transition, at temperatures near the critical temperature, our results will be reasonably insensitive to the temperature dependent variation of Δ in the superfluid phase. As we will see below, there is a very weak dependence of number of extra vortices on the correlation length (Eq.(8)), and hence on the temperature (Eq.(3)). Also, the observable effects of angular momentum from extra vortices will be significant only when the magnitude of the order parameter is a reasonable fraction of its zero temperature value, with the relevant time scale relating to the coarsening of string network. Thus, in our order of magnitude estimates, we will ignore the temperature dependence of Δ , and use its value at $T = 0$ as a typical value.

Here, we explore the effect on pulse modulation due to the formation of random vortex networks in the core, resulting from the normal to superfluid phase transition. This effect is determined by the number of net vortices, which depends on the coherence length ξ of the relevant thermodynamic phases. Estimates of the coherence length in BCS theory give a range of values for ξ depending on the Fermi momentum k_f of neutrons. For example, the authors of Ref. (Gezerlis et al. 2014) (see also, Ref. (Elgaroy & De Blasio 2001)) estimated the value of ξ in the range of a few tens fm to order 100 fm, as the neutron's Fermi momentum varies from 0.1 fm⁻¹ to 0.8 fm⁻¹. We will use a sample value of $\xi = 100$ fm for our purpose. We will see below that our results have a very weak dependence on the value of ξ .

2.2 Superfluidity in Color Superconducting Phases of QCD

There are suggestions that the core of a neutron star, at very high baryon chemical potential with low temperature, may host various exotic thermodynamic phases of QCD (Shifman & Ioffe 2000; Alford et al. 2001, 2008). These sug-

gestions follow from the realization that at very high values of baryon chemical potential, the physics should be governed by the low energy excitations near the Fermi level. In this case, the dynamics at the Fermi surface at $T \simeq 0$ is governed by the quarks and the gluon-mediated quark-quark interactions. The CFL phase may occur at ultra-high quark chemical potential of order 500 MeV, where $u, d,$ and s quarks can be treated massless. As suggested in the literature, this phase can occur if the NS core achieves an extreme mass density. For CFL phase, the attractive interaction between the quarks in (color antisymmetric) 3^* channel causes Fermi surface instability favouring diquarks BCS pairing, leading to the *color superconducting phase*. With color antisymmetric (3^* channel), spin antisymmetric (for 1S_0 pairing), the condensate should be flavor antisymmetric with the structure,

$$\langle q_i^\alpha q_j^\beta \rangle \sim \Delta_{CFL} (\delta_i^\alpha \delta_j^\beta - \delta_j^\alpha \delta_i^\beta) = \Delta_{CFL} \epsilon^{\alpha\beta n} \epsilon_{ijn} \quad (1)$$

where $\alpha\beta$ are flavor indices and ij are color indices. Note that the condensate is invariant under equal and opposite color and (vector) flavor rotations. Hence, it is called as color-flavor locked phase. It leads to the following spontaneous symmetry breaking pattern,

$$SU(3)_{color} \times SU(3)_L \times SU(3)_R \times U(1)_B \rightarrow SU(3)_{C+L+R} \times Z_2 \quad (2)$$

Thus, the $SU(3)_C$ color symmetry of QCD, along with three flavors chiral symmetry, is spontaneously broken. Fundamental group of the vacuum manifold here is Z , giving rise to vortices. Superfluid nature arises from the spontaneous breaking of $U(1)_B$. Depending on the relative mass difference between u, d and s quarks, other interesting phases at high baryon chemical potential may also appear in the core, namely, the $2SC$ phase for two light u and d quarks, or the LOFF phase, when chemical potential is not too large compared to the strange quark mass.

Observational signatures of these phases have been discussed in the literature (Alford et al. 2008; Rajagopal 2002). For example, the central core with CFL phase leads to suppressed cooling by neutrino emission and has smaller specific heat. Thus, the outer layer in the standard nucleonic phase will dominate NS's total heat capacity and neutrino emission with the CFL core. From the perspective of possible signatures of the exotic QCD phases, some of us in Ref. (Bagchi et al. 2015; Srivastava et al. 2017; Bagchi et al. 2022) suggested that the above symmetry breaking phase transitions may cause density fluctuations in the core by forming topological defects, leading to a transient change of moment of inertia (MI) tensors components. (Bagchi et al. 2015) have shown that the change of diagonal components of the MI tensor may lead to the change of the spin frequency of the pulsars and may be responsible for glitches and/or anti-glitches. The fluctuations being random, the generation of quadrupole moments may lead to the emission of gravitational waves. In the subsequent work (Bagchi et al. 2022), the authors have studied the effect of the development of the non-zero off-diagonal components of the MI tensor on pulse profile. Following the spirit of those works (Bagchi et al. 2015, 2022), here we shall explore the possibility of probing the superfluid phases (neutron superfluid and CFL) through the

observational effects on pulsars due to the formation of random topological vortices in the core implementing the suggested new mechanism of random vortex formation in Ref. (Das et al. 2017; Dave & Srivastava 2019).

For the estimate of coherence length ξ , we shall follow the Ref. (Iida & Baym 2002), where the coherence length has been estimated for the CFL phase within the Ginzburg-Landau theory in weak coupling limit as,

$$\xi = 0.26 \left(\frac{100 \text{ MeV}}{T_c} \right) \left(1 - \frac{T}{T_c} \right)^{-1/2} \text{ fm}. \quad (3)$$

The critical temperature T_c for CFL transition is related to the CFL gap Δ_0 at $T = 0$ through $T_c \simeq 0.57\Delta_0$. The value of Δ_0 lies in the range (40 - 90) MeV (See Refs. (Berges & Rajagopal 1999; Evans et al. 1999) for various issues related to estimating the superfluid parameters.), resulting in $T_c \simeq (20 - 50)$ MeV. The critical temperature T_c for CFL transition is too high compared to the typical star's temperature, favouring such phase at extremely high baryon density. The above values of T_c and T provide the coherence length ξ in the (0.5 - 1) fm range.

3 FORMATION OF RANDOM VORTEX NETWORK IN A SUPERFLUID TRANSITION

Here we will discuss how a superfluid phase transition leads to formation of a dense random vortex network. This random vortex network forms in addition to vortices needed to account for any initial rotation of the system. The formation of random network of vortices arises from the so called Kibble-Zurek mechanism (Kibble 1976, 1980; Zurek 1996). However, this mechanism needs modification to introduce a bias for the formation of extra vortices for the case when the system has initial rotation (Das et al. 2017; Dave & Srivastava 2019). We will discuss basic physics of these modifications needed. However, for the case at hand, we will find that the density of extra vortices arising from initial rotation is many orders of magnitude smaller than the random vortex network density arising from the usual Kibble-Zurek mechanism. Thus, for this case, one can get reasonable estimates by ignoring these modifications. However, we will discuss an important aspect of the formation of random vortex network from Refs. (Das et al. 2017; Dave & Srivastava 2019) which needs to be incorporated in the discussions of the Kibble-Zurek mechanism for prediction of observed effects of fluid circulation. This will involve implementation of local linear momentum conservation, for the random vortex network formation, and will lead to the conclusion that the flow generated for the superfluid component during formation of vortices be balanced by an equal and opposite momentum in the normal fluid. The end result will be that the arbitrarily oriented angular momentum component of the vortex network is finally transferred (with opposite direction) to the outer shell of neutron star.

Superfluid vortex is one example of topological defects. Topological defects arise in a wide range of systems. There are numerous examples of topological defects in condensed matter systems. It is also expected that certain topological defects arise in symmetry breaking transitions in the early universe. The first detailed theory of formation of topological

defects via a domain structure arising during a phase transition was proposed by (Kibble 1976, 1980) in the context of early universe. It was subsequently realized that this *Kibble mechanism* applies equally well to any symmetry breaking transition (Zurek 1996) (see also (Gupta et al. 2010, 2012; Mohapatra & Srivastava 2013)). This has allowed the possibility of testing the predictions of Kibble mechanism in various condensed matter systems, see Refs. (Hendry et al. 1994; Ruutu et al. 1996; Dodd et al. 1998; Carmi et al. 2000; Volovik 1996; Carmi et al. 2000; Maniv et al. 2003; Rivers & Swarup 2003; Kavoussanaki et al. 2000; Rudaz et al. 1999; Snyder et al. 1992; Chuang et al. 1993, 1991; Bowick et al. 1994; Ray & Srivastava 2004; Digal et al. 1999). There are important issues for defect formation in continuous transitions due to critical slowing down (Zurek 1996). The Kibble-Zurek mechanism incorporates these aspects and leads to specific predictions of the dependence of defect densities on the time scale of the phase transition.

An important aspect of the theory proposed by Kibble is that the basic mechanism has many universal predictions making it possible to use condensed matter experiments to carry out rigorous experimental tests of the predictions made for cosmic defects (Bowick et al. 1994; Ray & Srivastava 2004; Digal et al. 1999) in laboratory experiments. One of such universal predictions relates to the correlation between the formation of defects and anti-defects (Digal et al. 1999), and we will be using this specifically in our calculations below.

The crucial element of the theory proposed by Kibble is the recognition that phase transitions lead to formation of a sort of domain structure with the order parameter field varying randomly from one domain to another. Individual domains correspond to the correlation regions where order parameter field is taken to be roughly uniform. Second important input in this theory is the assumption that the order parameter field between two adjacent domains varies along the shortest path on the vacuum manifold. This is called as *the geodesic rule*. Its validity for different cases, such as those involving gauge symmetries, and possible violations in certain specific situations which are dominated by fluctuations has been discussed in the literature (Rudaz & Srivastava 1993; Digal et al. 1997). With these two physical inputs, one gets a geometrical picture for the physical region undergoing phase transition. One can then use straightforward topological arguments to calculate the probability of formation of defects and anti-defects at different junctions of domains. The probability of defect formation in this theory is calculated *per correlation domain* and it is a universal prediction, depending only on the underlying symmetries and space dimensions. This universality has allowed experimental test of the prediction of defect density in liquid crystal experiments (Bowick et al. 1994) (see also (Ray & Srivastava 2004; Digal et al. 1999)) for a first order transition case where correlation domains could be directly identified as bubbles of the nematic phase nucleating in the background of isotropic phase. For a continuous transition, effects of critical slowing down introduce dependence of relevant correlation length on the rate of phase transition (Zurek 1996). The Kibble-Zurek mechanism incorporates these considerations in prediction of defect density (Zurek 1996).

In the following, we will discuss basic elements of this theory for the specific case of spontaneous breaking of global $U(1)$ symmetry. This is the case for the superfluid transi-

tion for nucleon superfluidity, as well as for superfluidity in the CFL phase. Superfluid component is characterized by the condensate wave function, $\Psi = \Psi_0 e^{i\phi}$, where Ψ_0^2 gives number density of superfluid component and the phase ϕ is related to the superfluid velocity \vec{v}_s ,

$$\vec{v}_s = \frac{\hbar}{m} \vec{\nabla} \phi \quad (4)$$

Here m is the mass of the atomic unit which is condensing, for superfluid ^4He , it will be mass of ^4He atom, for our case of neutron superfluidity, it will be case the mass of Cooper pair of neutrons, hence $m = 2m_N$, m_N being mass of neutron. Superfluid vortices arise where the phase ϕ winds non-trivially, we may call vortex as those points around which net variation of ϕ is $+2\pi$ with anti-vortex corresponding to -2π variation of ϕ . (Similarly, for higher windings with multiples of 2π .) The order parameter space in this case is a circle S^1 . According to Kibble's theory, defects form due to the domain structure arising in the phase transition. The domains here will be characterized by roughly uniform ϕ which varies randomly from one domain to another. In accordance to the geodesic rule, ϕ will vary with least gradient in between adjacent domains. By considering the probability of finding a non-zero (± 1) winding around a junction of three domains, one can show (Bowick et al. 1994; Ray & Srivastava 2004) that the probability of vortex/antivortex formation per domain, in two space dimensions, is equal to $1/4$. This can be straightforwardly generalized to three space dimensions where one gets vortex line (topological string) defects. Simulations show that the average number of strings per correlation domain is 0.88 (Vachaspati & Vilenkin 1984). Interestingly, the statistical properties of initial string network are universal, with strings basically forming Brownian trajectories with persistence length of the correlation length. There are large number of string loops, while many strings stretch across the system.

Vortex here corresponds to positive circulation of fluid, with anti-vortex corresponding to opposite circulation. As we are interested in net angular momentum, we need to find net vortex – antivortex number which are ending at a given surface. This will give net angular momentum perpendicular to that surface. An important point here is that one needs to know here the angle at which a given vortex or antivortex ends at the surface. That will give the direction of angular momentum carried by the vortex/antivortex at that surface. We will be using primarily topological arguments, which will only give probability of non-zero winding at the surface. Detailed simulation like in Ref. (Vachaspati & Vilenkin 1984) can give the information of the angle. However, this will only contribute to a factor of order one. As we will see, in our estimates, factors of order one will be completely irrelevant, hence we will not worry about this issue.

One may expect that if N is the net number of vortices plus antivortices ending at a surface, then the number of vortices minus number of antivortices, ΔN will typically be of order \sqrt{N} . This, however, is not true. The underlying domain structure induces certain correlation between vortices and antivortices (Digal et al. 1999), due to which ΔN is strongly suppressed. In fact, domain structure directly allows us to calculate ΔN for any given area. Consider a 2-dimensional surface S which has area A , and perimeter length L . The perimeter will consist of L/ξ number of correlation domains, where ξ

is the correlation length. With ϕ varying randomly from one domain to another, we essentially have here a random walk problem for ϕ where the average step size for ϕ is $\pi/2$ (as the largest variation in ϕ step is π and the shortest is zero). We can then conclude that the net winding of ϕ , as we go around the perimeter L , (which will give the net vortex minus anti-vortex number ΔN enclosed within L), will be distributed about zero with a typical width $\sigma = \frac{\pi/2}{2\pi} \sqrt{\frac{L}{\xi}} = \frac{1}{4} \sqrt{\frac{L}{\xi}}$. The total number of vortices plus anti-vortices N is proportional to the area A (with a fixed probability of vortex/antivortex per domain, which is equal to $1/4$ for 2 space dimensions for this case). Thus, we conclude that $\sigma \propto N^{1/4}$ which is in complete contrast to the naive expectation of the Poisson distribution for ΔN with width \sqrt{N} . We thus get a scaling relation for σ :

$$\sigma = CN^\nu \quad (5)$$

The exponent ν is universal here with a value of $\nu = 1/4$ for the case of vortices with spontaneous breaking of $U(1)$ symmetry. We again emphasize, this highly non-trivial prediction arises from the underlying domain structure in this picture of vortex formation, and is in complete contrast to naive expectation of $\nu = 1/2$ for random sprinkling of vortices and anti-vortices. The constant C is not universal and depends on details like shapes of elementary correlation domain etc. Typically its value is of order 1 (e.g. $C = 0.57$ and 0.71 for triangular and square domains respectively), and as mentioned above, factors of order 1 will be completely irrelevant in our present case, as we will see below.

The prediction of the distribution of ΔN being centered at zero (and with σ) is for the case when vortices form in a system which has no initial rotation. For a rotating system, a network of vortices (vortex lattice) has to finally form which carries the initial angular momentum. These extra vortices will be in addition to the vortex network formed via the Kibble-Zurek mechanism. Thus the basic picture of Kibble-Zurek mechanism has to be modified so that extra vortices are produced during the transition in accordance to the initial angular momentum of the system. A detailed investigation of this was carried out in Ref.(Das et al. 2017; Dave & Srivastava 2019) where it was shown that it requires modification of both crucial elements of the Kibble's basic picture of defect formation via domains. Order parameter within a correlation domain can no longer be assumed to be roughly constant, indeed ϕ must vary everywhere in accordance to the initial rotation velocity of the fluid (which becomes rotation velocity of the superfluid). Further, the geodesic rule also gets modified as ϕ variation within correlation domains has a non-trivial space dependence. This affects the entire distribution of defects, and hence also the distribution of ΔN (though the effect on σ is small). We refer the reader to Ref.(Das et al. 2017; Dave & Srivastava 2019) for these details. However, in the present case, typical separation between vortices/anti-vortices formed during transition will be of order the correlation length, ranging from 1 fm to 100 fm for CFL vortices or neutron superfluid vortices respectively, whereas typical inter-vortex separation arising from initial rotation of neutron star is of order 0.1 mm. This implies that number of extra vortices will be many orders of magnitude smaller than the number of vortices/antivortices

formed during the phase transition (about 18 to 20 orders of magnitude smaller). Thus, we can safely neglect effect of initial rotation on the basic mechanism of vortex formation here, and will continue to use the estimate of σ as given in Eq.(5). We mention here that the modification of the Kibble mechanism due to effects of initial rotation becomes important only when order parameter variation in each domain is significantly modified. This happens only when the net vortex number (number of vortices minus number of antivortices) becomes a reasonable fraction of the total number of vortices (vortices plus antivortices), which is not the case here (see Ref.(Dave & Srivastava 2019) for details).

However, there is one important aspect of superfluid vortex formation which needs to be incorporated in discussions of Kibble-Zurek mechanism, especially in relation to the experimental observations of fluid flow development during the transition. (See, (Das et al. 2017; Dave & Srivastava 2019) for a detailed discussion of this). During phase transition, the spontaneous generation of flow of the superfluid due to vortex formation in some region means that some fraction of neutrons (or diquarks for the CFL case) form the superfluid condensate during the transition and develop momentum due to the non-zero gradient of the phase of the condensate. The remaining neutrons (or quarks, which form the normal component of fluid in the two-fluid picture) will then develop opposite linear momentum so that the linear momentum is local conserved. This implies that the normal fluid around each vortex formed should develop a flow which is exactly the same but opposite to the profile of the superfluid velocity of the vortex, depending on relative fraction of the normal fluid and the superfluid. (As emphasized in Refs.(Das et al. 2017; Dave & Srivastava 2019), these arguments show that during superfluid transition, as vortices form, superflow and normal flow will have initial opposite directions, so experimental detection will be complicated, unless one finds a way to distinguish between normal flow and superflow, e.g. with flow evolution due to viscous effects of the normal flow).

In our present case, the above discussion has very important implication. As the neutron star core undergoes superfluid transition, random vortex network will form which will impart an arbitrarily oriented net angular momentum to the superfluid of the core (in addition to the angular momentum coming from the initial rotation of the core). However, the superfluid part is decoupled from rest of matter in the neutron star, so this additional random angular momentum does not transfer to the outer shell of the neutron star. (Note, the situation is different for the initial angular momentum. Initially, the entire neutron star is rotating, including the outer shell, neglecting any differential rotation. Even though the core becomes superfluid, and decouples from rest of the matter, apart from the pinning of vortices, the shell has same rotation velocity in the beginning.) However, in view of the above arguments of local linear momentum conservation, we conclude that the normal matter in the neutron star will develop an angular momentum which is equal and opposite to the net randomly oriented angular momentum arising from the vortex network formed during the transition. This will be transferred to the shell and should be observable in perturbations of the pulses of the pulsar. In the next section we will make estimate of this extra angular momentum.

4 ESTIMATES OF EXTRA ANGULAR MOMENTUM ARISING FROM THE RANDOM VORTEX NETWORK

The basic picture of random vortex network formation discussed above can now be used to estimate any extra angular momentum arising from this network. We will take neutron star with radius of 10 km, and will consider a spherical core region with radius R_c which undergoes superfluid phase transition. R_c can be as large as about 9 km for nucleon superfluidity, while for extreme baryon density QCD phases (e.g. CFL phase) it may be 5 km or less. As the superfluid transition proceeds, two sets of vortices will form. One set will arise from the initial rotation of the fluid, which will lead to a relatively dilute system of vortices (with typical inter-vortex spacing of about 0.1 mm). The second vortex set is of interest to us, and it consists of vortices/antivortices formed via the Kibble-Zurek mechanism. This will be an extremely dense network of vortex line defects which will have initial shape of Brownian trajectories, with some ending at the surface of the core region of radius R_c , while most will form closed loops entirely enclosed within this region. (See, (Vachaspati & Vilenkin 1984) for the universal features of the statistical distribution of such string defects.) Typical separation between vortex/antivortex line defects will be of order of the correlation length ξ for the superfluid phase transition. It is important to note here that the only relevant detail of the specific model of superfluid phase transition here is the correlation length ξ . Everything else will be entirely determined in terms of ξ . We will take sample values of $\xi \sim 1$ fm for the superfluidity in the color superconducting QCD phase (e.g. CFL phase) (Iida & Baym 2002), and $\xi \sim 100$ fm for the conventional neutron superfluid case. Again, we will see, that factors of order one will be irrelevant to our estimates.

As discussed above, the density of vortices arising from the initial rotation is many orders of magnitude smaller than the density of vortices formed via the Kibble-Zurek mechanism. Therefore, we will ignore any effects of rotation on the Kibble-Zurek mechanism (which requires modifications for a rotating system as discussed in Ref.(Das et al. 2017; Dave & Srivastava 2019)). We further note that any vortex loop which is entirely enclosed within the core region of size R_c does not contribute to any net angular momentum for the core. If at all, it can contribute to localized patterns in the fluid flow. However, any vortex/antivortex ending at the surface of the superfluid core region will contribute to a net angular momentum. The total angular momentum of the superfluid core region can be found by simply adding contributions coming from all vortices and antivortices ending at different points on the surface of this spherical core region with radius R_c .

As vortices and anti-vortices contribute to opposite fluid circulations, clearly the quantity of interest to us is the net vortex number $\Delta N = \text{vortex number} - \text{anti-vortex number}$. As we explained in Section II, ΔN is distributed about zero with typical width of σ . σ is given in Eq.(5) as calculated using the domain structure underlying the Kibble-Zurek mechanism. Again, we neglect any effect of initial rotation on this calculation of ΔN , and σ , first due to extremely dilute system of vortices arising from initial rotation, and secondly that modified Kibble-Zurek mechanism shows very weak de-

pendence of the exponent ν on the system rotation (Das et al. 2017; Dave & Srivastava 2019).

To use Eq.(5) for estimating typical net vortex number ΔN , we need to use a 2-dimensional region of area A . The relevant 2-dimensional surface for us is the surface of the spherical core region with radius R_c . However, here we note a problem as this surface is a closed manifold, forming a 2-sphere S^2 . A closed manifold necessarily introduces correlations between vortices and antivortices ending at the surface, as every vortex ending at one point on this surface of S^2 has to have an exit point on this S^2 . The estimate of σ in Eq.(5) does not incorporate such correlations. However, we will ignore this complication using the following justification. As vortex strings form typical Brownian trajectories, with persistence length of ξ (which is in the range of 1 - 100 fm), it is extremely unlikely for a given vortex to continue all the way to the opposite end of the surface of S^2 which has a radius of about 5 - 9 km. Most often such a vortex will bend around quickly and will end at some point on S^2 , not too far from the initial point, (where it will exit as an anti-vortex). Thus, the surface of S^2 with a radius of 5-9 km can be viewed as consisting of smaller patches (still, orders of magnitude larger than ξ), and the estimate of σ in Eq.(5) can be applied to each such patch, while ignoring the fact that all these patches are eventually glued to form a closed manifold. (For a proper check of these arguments, one needs to carry out detailed simulation of string formation in a spherical region S^2 , with open boundary conditions, which allow windings to form on the surface of this S^2 , which extend to string defects in the interior region. This is non-trivial as typically one performs simulations with periodic, or closed (fixed), boundary conditions. We hope to carry out such a simulation in a future work.)

It is important to note that this argument cannot be used for the net vortex number which arises from the initial rotation of the system. As we explained above, initially rotating system must ensure that finally there is a required net vortex number (vortices minus antivortices) in the direction of initial rotation (which will be ensured by a suitably modified Kibble mechanism (Dave & Srivastava 2019)). Thus, even with Brownian trajectories of vortices with a very small step-size, correct number of net vortices will be ensured right in the beginning of vortex formation, when the order parameter is settling down to its superfluid phase value. The extra vortices we have calculated, arise at a later stage when superfluid phase is established, and gradient energies arising with application of geodesic rule have resulted in appropriate superfluid flow (with normal fluid developing opposite flow, as explained earlier).

With these points clarified, rest of the calculations are straightforward. Net number of correlation domains on the surface of S^2 with radius R_c is given by:

$$N_{\text{domains}} \simeq \frac{4\pi R_c^2}{\xi^2} \quad (6)$$

Typical value of ΔN is characterized by σ in Eq. (5). We thus estimate typical value of net vortex number as

$$\Delta N \sim \sigma = CN^{1/4} = C (4\pi)^{1/4} \sqrt{\frac{R_c}{\xi}} \quad (7)$$

We now note that these extra vortices will be roughly uni-

formly distributed on the entire surface of S^2 which is the boundary of the superfluid core region. A vortex will contribute to positive angular momentum along local perpendicular direction. (Again as we discussed earlier, any inclination of the angular momentum arising from the angle of the vortex string ending at the surface will contribute to factor of order 1 which will be immaterial here.) Thus, on the average, equal number of vortices will exit in positive x direction, and negative x direction, similarly for y and z directions. Thus, one may expect roughly $\sigma/6$ number of vortices to typically exit along a given direction, (with roughly equal number on average to exit in the opposite direction, and same in other two directions). However, this is only on average, there will be statistical fluctuations, and in this case, distribution of these extra vortices will be expected to follow Poisson distributions as the domain structure introduces no further evident restrictions on how these extra vortices are distributed. (Validity of this expectation needs to be checked by detailed numerical simulations). We thus conclude that after all the cancellations of opposite circulations (due to the extra vortices exiting in different directions), one will expect a net number N_{net} vortices to point along some specific direction, which should be typically of order

$$N_{net} \sim \sqrt{\frac{\sigma}{6}} = \sqrt{\frac{C}{6}} N^{1/8} = \sqrt{\frac{C}{6}} (4\pi)^{1/8} \left(\frac{R_c}{\xi}\right)^{1/4} \quad (8)$$

With C being of order 1, N_{net} is entirely determined by the last factor of $(R_c/\xi)^{1/4}$. Further, core size of $R_c = 5$ or 9 km also makes no difference. We take $R_c = 9$ km. With that we find $N_{net} \simeq 10^4$ for $\xi = 100$ fm (for neutron superfluid case), and $N_{net} \simeq 10^5$ for $\xi = 1$ fm (for superfluidity in the color superconducting case). Here we have ignored factors of order 1.

We now recall from the discussion at the end of previous section, that this extra angular momentum of superfluid vortices has to be counter balanced by the generation of same, but opposite, angular momentum in the normal fluid component due to local linear momentum conservation. Thus, we conclude that during superfluid transition in a spherical region of radius $R_c \simeq 5 - 9$ km, a net angular momentum will be generated which will be pointing in an arbitrary direction, completely uncorrelated to the original direction of rotation of the neutron star. The magnitude of this angular momentum will be equal to the angular momentum carried by about 10^4 to 10^5 superfluid vortices in this spherical region, the two numbers corresponding to the neutron superfluid case, and superfluidity in superconducting QCD phase, respectively.

5 OBSERVATIONAL EFFECTS, PULSE TIMING AND PULSE PROFILE CHANGES

We now estimate the value of the angular momentum arising from these net vortices, pointing in an arbitrary direction at the surface of the superfluid core of radius R_c . Quantization of the circulation around a superfluid vortex means that the angular momentum of each Cooper pair for a vortex (with unit circulation) is \hbar . Thus, net angular momentum arising from N_{net} number of vortices is

$$L_{vortex} = \hbar N_{net} \left(\frac{M_{SF}}{m_{pair}}\right) \quad (9)$$

Here M_{SF} is the mass of the superfluid component of the core. There is a range of estimates of M_{SF} in the literature (Jones 2010; Sourie & Chamel 2020) varying from few percent to almost 80 % of the neutron star mass. For rough estimates, we will take $M_{SF} \sim M_{sun} \simeq 10^{33}$ grams. m_{pair} is the mass of the Cooper pair which will be equal to $2m_{neutron}$ for neutron superfluidity, while $m_{pair} \simeq m_{diquark} \simeq$ few hundred MeV for the color superconductivity occurring at very high baryonic chemical potential. Again, for rough estimates, we will take $m_{pair} = 2$ GeV for both cases. To represent a general case, we consider the situation when L_{vortex} points in a direction transverse to the direction of the original angular momentum L_0 which we take to be along the z axis. With this extra angular momentum, the outer shell now has the net angular momentum pointing in a direction which is tilted by an angle θ w.r.t the z axis. We take L_0 to be

$$L_0 \simeq 10^{45} (\text{g cm}^2) \frac{2\pi}{T_0} \quad (10)$$

where $T_0 (= \frac{2\pi}{\omega_0})$ is the initial time period (in sec.) of the rotation of the neutron star. With this, the angle θ will be given by (for $L_{vortex} \ll L_0$)

$$\theta \simeq \frac{L_{vortex}}{L_0} = \frac{\hbar N_{net} \left(\frac{M_{SF}}{m_{pair}}\right)}{10^{45} (\text{g cm}^2) \omega_0} \simeq N_{net} T_0 10^{-16} \quad (11)$$

For millisecond pulsars, we get values of θ as 10^{-15} to 10^{-14} for the two cases of superfluidity. For slow rotating pulsar, with $T_0 \sim 1$ sec. $\theta \simeq 10^{-12}$ to 10^{-11} for the two cases.

For observational effects, we consider specific case of the pulsar having shape of an oblate spheroid, initially rotating about the principal symmetry axis z . We take $I_{zz} > I_{xx} = I_{yy}$ with oblateness of the pulsar characterized by $\eta = \frac{I_{zz} - I_{yy}}{I_{zz}}$. With extra angular momentum leading to the tilting of net angular momentum away from the principal symmetry axis z , pulsar will begin to wobble, with the wobbling frequency Ω given by

$$\Omega \simeq \eta \omega_0 \quad (12)$$

where $\omega_0 = 2\pi/T_0$ is the initial angular frequency of rotation. The structure of modulated pulses can be calculated straightforwardly using Euler's equations (see, e.g. Ref. (Bagchi et al. 2022)). The angular amplitude of wobbling will be given by

$$\theta_{wobble} \simeq \theta \frac{\omega_0}{\Omega} \simeq \frac{\theta}{\eta} \quad (13)$$

Neutron stars typically have very small values of η . Taking a sample value of $\eta \sim 10^{-6}$ we find angular amplitude of wobble to be about 10^{-5} to 10^{-6} for the cases of CFL superfluidity and neutron superfluidity respectively. This should be detectable in observations of pulse modifications.

For the cases when L_{vortex} is along the initial rotation axis (z axis), it will appear as a glitch, suddenly increasing the rotation frequency, or decreasing it, which will then appear as anti-glitch. Note that this gives the correct range of glitch amplitude as we will get

$$\frac{\delta\omega}{\omega} = \frac{L_{vortex}}{L_0} \quad (14)$$

This can range from 10^{-15} to 10^{-11} as shown above. Further, this extra angular momentum does not have to vanish at the end of the coarsening of the vortex network. Importantly, in this picture, one gets a unified explanation of glitches and anti-glitches which correspond to L_{vortex} being along the direction of L_0 , or opposite to it, respectively. Note that we are not implying that this mechanism can provide explanation of all glitches and anti-glitches. First, in our mechanism, glitches/anti-glitches will occur in neutron stars which are undergoing superfluid transition. However, glitches have been observed in very old pulsars with internal temperatures much lower than the superfluid critical temperature. Further, glitches have been observed multiple times in certain pulsars, which will be very hard to accommodate in the present scenario. Also, glitches with much larger magnitudes have been observed, than the magnitudes estimated here. Thus, as far as glitches/anti-glitches are concerned, the present mechanism may only be able to account for some of them, and one has to invoke other very established mechanisms for most of these. The present mechanism should be considered as providing a new phenomenon, and its observational effects should have distinct features compared to the other mechanism which are needed to explain a large range of glitches and anti-glitches which have been observed.

An extremely important aspect of our model is that it predicts a universal behavior of changes in the rotational dynamics of pulsar. L_{vortex} arises from the random vortex network formed during the superfluid phase transition. The decay of this network follows universal scaling laws. For example, for the 2-d case, vortex number scales as $t^{-\zeta}$ where ζ may be 1 or 1/3 depending on the nature of vortex-antivortex interaction (Brandenberger 1994; Liu et al. 2021). The observational effects of the random vortex network are all proportional to L_{vortex} which is determined by the net number of extra vortices N_{net} exiting the surface of S^2 in certain direction. Eq.(8) shows that N_{net} is proportional to $N^{1/8}$, with N being the total number of vortices and anti-vortices. With N decaying as a power law, we expect that L_{vortex} will decay as a power law $t^{-\zeta/8}$. Note, the net vortex number here can change as vortices exiting the surface of S^2 in different directions will re-orient during evolution. Thus vortices on the surface of S^2 can slide and can annihilate oppositely oriented vortices in different directions. In general, due to curved surface of S^2 , one should expect very few extra vortices to survive, only those which stretch along the direction of rotation of the star. As we mentioned, this will be consistent with the behavior of glitches/anti-glitches where the initial angular momentum is not fully restored. During this coarsening of vortex network, all observational effects, from wobbling frequency, to wobbling amplitude, and the amplitudes of glitches/anti-glitches will be expected to decay with this power law. This will be a unique distinguishing signal of the applicability of our model, and a direct signal of superfluid phase transition occurring inside a pulsar core.

6 CONCLUSION

We have considered the case of a superfluid phase transition occurring in the core of a pulsar and have studied observational effects of the random vortex network formed via the Kibble-Zurek mechanism during the transition. Due to these vortices, extra angular momentum is generated for the outer shell of the pulsar which can point in any arbitrary direction. This leads to wobbling of the pulsar, along with possibility of glitches/anti-glitches depending on the relative direction of this extra angular momentum and the original angular momentum of the pulsar. Importantly, the prediction of our model are almost universal, entirely characterized by the symmetry breaking (U(1) in this case), and the superfluid correlation length. Further, the observational effects on the perturbations in the rotational dynamics of the pulsar should decay in accordance with specific power law determined by power law decay of the vortex network formed in the phase transition. These universal features can help in identifying the nature of phase transition occurring inside a pulsar core.

There are important aspects of our model which need further investigations. The decay of vortex network will lead to annihilation of vortices/antivortices at the surface of S^2 . This dynamics will be complicated due to curved nature of the surface as vortices exiting in different directions can slide on the surface and annihilate/join with the vortices at different points. A proper study of this can only be done by a detailed numerical simulation of the evolution of vortex network. Even the calculation of net extra angular momentum pointing in certain direction (with our assumption of applicability of Eq.(5) for different patches of the surface of S^2) needs to be verified with a detailed simulation. We plan to carry out such a simulation to address these issues. We have ignored any discussion of the superconductivity arising from the Cooper pairing of protons in the neutron star core. All our arguments can be straightforwardly extended to this superconducting phase. Its implications will be very interesting as string defects will now be magnetic flux tubes, hence extra vortices will imply changes in the magnetic field of neutron star. This will clearly have distinct observational signatures, and needs to be further explored.

7 ACKNOWLEDGMENTS

We thank Shreyansh S. Dave and Arpan Das for useful discussions. Partha Bagchi acknowledges the financial support from Department of Atomic Energy (DAE) project RIN 4001.

8 DATA AVAILABILITY

No new data were generated or analysed in support of this research.

References

- Alford M., Bowers J., Rajagopal K., 2001, *Journal of Physics G: Nuclear and Particle Physics*, 27, 541
- Alford M. G., Schmitt A., Rajagopal K., Schäfer T., 2008, *Rev. Mod. Phys.*, 80, 1455
- Allard V., Chamel N., 2024, *Phys. Rev. Lett.*, 132, 181001

- Anderson P. W., Itoh N., 1975, *Nature*, 256, 25
- Antonopoulou D., Haskell B., Espinoza C. M., 2022, *Rept. Prog. Phys.*, 85, 126901
- Bagchi P., Das A., Layek B., Srivastava A. M., 2015, *Phys. Lett. B*, 747, 120
- Bagchi P., Layek B., Sarkar A., Srivastava A. M., 2022, *Mon. Not. Roy. Astron. Soc.*, 513, 2794
- Bauswein A., Bastian N.-U. F., Blaschke D. B., Chatziioannou K., Clark J. A., Fischer T., Oertel M., 2019, *Phys. Rev. Lett.*, 122, 061102
- Baym G., Pethick C., Pines D., 1969, *Nature*, 224, 673
- Berges J., Rajagopal K., 1999, *Nuclear Physics B*, 538, 215
- Bowick M. J., Chandar L., Schiff E. A., Srivastava A. M., 1994, *Science*, 263, 943
- Brandenberger R. H., 1994, *Int. J. Mod. Phys. A*, 9, 2117
- Carmi R., Polturak E., Koren G., 2000, *Phys. Rev. Lett.*, 84, 4966
- Chuang I., Yurke B., Durrer R., Turok N., 1991, *Science*, 251, 1336
- Chuang I., Yurke B., Pargellis A. N., Turok N., 1993, *Phys. Rev. E*, 47, 3343
- Das A., Dave S. S., De S., Srivastava A. M., 2017, *Mod. Phys. Lett. A*, 32, 1750170
- Dave S. S., Srivastava A. M., 2019, *EPL (Europhysics Letters)*, 126, 31001
- Dean D. J., Hjorth-Jensen M., 2003, *Reviews of Modern Physics*, 75, 607
- Demircik T., Ecker C., Järvinen M., Rezzolla L., Tootle S., Topolski K., 2022, *EPJ Web Conf.*, 274, 07006
- Digal S., Sengupta S., Srivastava A. M., 1997, *Phys. Rev. D*, 55, 3824
- Digal S., Ray R., Srivastava A. M., 1999, *Phys. Rev. Lett.*, 83, 5030
- Dodd M. E., Hendry P. C., Lawson N. S., McClintock P. V. E., Williams C. D. H., 1998, *Phys. Rev. Lett.*, 81, 3703
- Elgaroy O., De Blasio F. V., 2001, *Astronomy & Astrophysics*, 370, 939
- Evans N., Hsu S. D., Schwetz M., 1999, *Nuclear Physics B*, 551, 275
- Gezerlis A., Pethick C. J., Schwenk A., 2014, in , *Novel Superfluids: Volume 2*. Oxford University Press, p. 580, doi:10.1093/acprof:oso/9780198719267.003.0011
- Gupta U. S., Mohapatra R. K., Srivastava A. M., Tiwari V. K., 2010, *Phys. Rev. D*, 82, 074020
- Gupta U. S., Mohapatra R. K., Srivastava A. M., Tiwari V. K., 2012, *Phys. Rev. D*, 86, 125016
- Haskell B., Melatos A., 2015, *Int. J. Mod. Phys. D*, 24, 1530008
- Heiselberg H., Hjorth-Jensen M., 1998, *Phys. Rev. Lett.*, 80, 5485
- Hendry P. C., Lawson N. S., Lee R. A. M., McClintock P. V. E., Williams C. D. H., 1994, *Nature*, 368, 315
- Ho W. C. G., Heinke C. O., 2009, *Nature*, 462, 71
- Hughes J. P., Rakowski C. E., Burrows D. N., Slane P. O., 2000, *The Astrophysical Journal*, 528, L109
- Iida K., Baym G., 2002, *Phys. Rev. D*, 66, 014015
- Jones D. I., 2010, *Mon. Not. Roy. Astron. Soc.*, 402, 2503
- Kavoussanaki E., Monaco R., Rivers R. J., 2000, *Phys. Rev. Lett.*, 85, 3452
- Kibble T. W. B., 1976, *J. Phys. A*, 9, 1387
- Kibble T. W. B., 1980, *Phys. Rept.*, 67, 183
- Liu X.-P., et al., 2021, *Phys. Rev. Lett.*, 126, 185302
- Manchester R. N., 2017, *J. Phys. Conf. Ser.*, 932, 012002
- Maniv A., Polturak E., Koren G., 2003, *Phys. Rev. Lett.*, 91, 197001
- Migdal A., 1959, *Nuclear Physics*, 13, 655
- Mohapatra R. K., Srivastava A. M., 2013, *Phys. Rev. C*, 88, 044901
- Most E. R., Papenfort L. J., Dexheimer V., Hanauske M., Schramm S., Stöcker H., Rezzolla L., 2019, *Phys. Rev. Lett.*, 122, 061101
- Page D., Geppert U., Weber F., 2006, *Nuclear Physics A*, 777, 497
- Page D., Prakash M., Lattimer J. M., Steiner A. W., 2011, *Phys. Rev. Lett.*, 106, 081101
- Radice D., Bernuzzi S., Del Pozzo W., Roberts L. F., Ott C. D., 2017, *Astrophys. J. Lett.*, 842, L10
- Rajagopal K., 2002, *Color Superconductivity*. Springer Netherlands, Dordrecht, p. 475, doi:10.1007/978-94-010-0267-7_16
- Ray R., Srivastava A. M., 2004, *Phys. Rev. D*, 69, 103525
- Rivers R. J., Swarup A., 2003, *The Efficiency of Defect Production in Planar Superconductors and Liquid Crystals* (arXiv:cond-mat/0312082)
- Rudaz S., Srivastava A. M., 1993, *Modern Physics Letters A*, 08, 1443
- Rudaz S., Srivastava A. M., Varma S., 1999, *International Journal of Modern Physics A*, 14, 1591
- Ruderman M., 1976, *The Astrophysical Journal*, 203, 213
- Ruutu V. M. H., et al., 1996, *Nature*, 382, 334
- Sedrakian A., Clark J. W., 2019, *The European Physical Journal A*, 55, 167
- Shifman M., Ioffe B., eds, 2000, *The Condensed matter physics of QCD*. World Scientific, p. 2061 (arXiv:hep-ph/0011333), doi:10.1142/9789812810458_0043
- Shternin P. S., Yakovlev D. G., Heinke C. O., Ho W. C. G., Patnaude D. J., 2011, *Mon. Not. Roy. Astron. Soc.: Letters*, 412, L108–L112
- Shternin P. S., Ofengeim D. D., Heinke C. O., Ho W. C. G., 2022, *Mon. Not. Roy. Astron. Soc.*, 518, 2775
- Snyder R., Pargellis A. N., Graham P. A., Yurke B., 1992, *Phys. Rev. A*, 45, R2169
- Sourie A., Chamel N., 2020, *Mon. Not. Roy. Astron. Soc.*, 493, L98
- Srivastava A. M., Bagchi P., Das A., Layek B., 2017, *Pramana*, 89, 68
- Vachaspati T., Vilenkin A., 1984, *Phys. Rev. D*, 30, 2036
- Volovik G. E., 1996, *Czechoslovak Journal of Physics*, 46, 3048
- Yakovlev D. G., Pethick C. J., 2004, *Ann. Rev. Astron. Astrophys.*, 42, 169
- Yakovlev D., Gnedin O., Gusakov M., Kaminker A., Levenfish K., Potekhin A., 2005, *Nuclear Physics A*, 752, 590
- Zurek W. H., 1996, *Phys. Rept.*, 276, 177

This paper has been typeset from a $\text{\TeX}/\text{\LaTeX}$ file prepared by the author.